Applied Catalysis B: Environmental 138–139 (2013) 84–94

Contents lists available at SciVerse ScienceDirect

Applied Catalysis B: Environmental

journal homepage: www.elsevier.com/locate/apcatb

Fabrication, characterization and photocatalytic activity of TiO_2 layers prepared by inkjet printing of stabilized nanocrystalline suspensions

Marcela Černá[a], Michal Veselý[a], Petr Dzik[a,*], Chantal Guillard[b], Eric Puzenat[b], Martina Lepičová[a]

[a] BrnoUniversity of Technology, Faculty of Chemistry, Purkynova 118, 612 00 Brno, Czech Republic
[b] Institut of Recherches sur la Catalyse et l'Environnement de Lyon, CNRS UMR 5256, Universite de Lyon, 2 Avenue Albert Einstein, Villeurbanne F-69622 cedex, France

ARTICLE INFO

Article history:
Received 22 October 2012
Received in revised form 11 February 2013
Accepted 18 February 2013
Available online 27 February 2013

Keywords:
Photocatalytic activity
Hydrothermal synthesis
Inkjet printing
Colloidal dispersion

ABSTRACT

Titanium dioxide (TiO_2) colloidal dispersions were synthesized by hydrothermal synthesis in acidic pH under various process conditions. Phase structure of prepared TiO_2 was identified as pure rutile by X-ray diffraction analysis and crystallite sizes determined by the Scherrer equation were in the range of 10–25 nm. These values correlated with particle sizes observed by transmission electron microscopy (TEM). Afterwards, the prepared TiO_2 dispersions were used for the formulation of stable inkjet printable "inks". Thin layers of nanocrystalline TiO_2 were deposited by inkjet printing onto soda-lime glass substrates. After sintering at 500 °C, thin patterned films were obtained. Their basic physicochemical properties were characterized by standard methods. Optical microscopy and SEM imaging revealed highly structured topography of samples surface. Layer hardness was equivalent to the B pencil as determined by the "Pencil Hardness Test". The topology and roughness were examined by atomic force microscopy and RMS roughness was in the range of 40–100 nm. Band gap energy of TiO_2 determined by UV–vis reflection spectroscopy was consistent with known rutile values. The photocatalytic activity of printed layers was evaluated on the basis of 2,6-dichloroindophenoldiscoloration rate monitored by UV–vis spectroscopy and did not exceed the performanceof Aeroxide P-25. Despite average photocatalytic performace of this particular TiO_2 type, inkjet printing proved to be an efficient method for the fabrication of patterned titania films originating from nanocrystalline precursor.

1. Introduction

Heterogeneous photocatalysis being a promising water and air purification technique, has attracted a great deal of attention in the last years [1–6]. The main advantage of this method compared to the traditional wastewater treatment, such as chlorination or ozonolysis is that a lot of persistent contaminants, (e.g. phenol, 4-chlorophenol, trichloroethylene and chlorobenzene) can be completely mineralized including their potentionally problematic degradation byproducts [7–9]. Among various oxide semiconductorsefficient for photocatalysis, titanium dioxide is the bestphotocatalyst because of its strong oxidizing power, nontoxicity and relatively long-term photostability [10].

Absorption of UV light causes the generation pair of an electron and a hole. The excited electrons are trapped by O_2 to form superoxide radical ion (O_2). The holes can react with adsorbed water to form reactive hydroxyl radicals (•OH). These radicals are considered to be the major active species responsible for the photocatalytic oxidation reaction. These hydroxyl radicals can by quantitatively detected by photoluminescence [11].

Three main different crystalline phases of titanium dioxide exists: anatase (tetragonal), rutile (tetragonal) and brookite (orthorhombic). However, only anatase and rutile have been used in most photocatalytic studies and the photocatalytic activity of amorphous titania is negligible [12]. Anatase phase shows a higher photocatalytic activity than rutile due to its lower recombination rate of photo-generated electrons and holes [13,14].

It is well known that the photocatalytic activity of TiO_2 strongly depends on the preparation methods and post-treatment conditions, since they both have a decisive influence on the chemical and physical properties of TiO_2 [15–16]. Many approaches to improve the photocatalytic activity of TiO_2have been proposed. Generally, modification of its morphology, crystal composition, crystallinity, and surface area are the most common [17–24]. Of these approaches, hydrothermal treatment is one of the most widely used methods for increasing the crystallinity of TiO_2 [25,26].

The hydrothermal method of TiO_2 particles preparation has many advantages. A major advantage of using the hydrothermal

* Corresponding author. Tel.: +420 541 149 411; fax: +420 541 211 697.
E-mail address: petr@dzik.cz (P. Dzik).

0926-3373/$ – see front matter © 2013 Elsevier B.V. All rights reserved.
http://dx.doi.org/10.1016/j.apcatb.2013.02.035

process is the ability to produce different crystalline phases without the need of subsequent thermal treatment as it provides the capacity to grow good-quality crystals and to control the crystalline composition simultaneously [27]. By changing the hydrothermal reaction conditions, such as the reaction temperature, pH values, reactant concentrations and molar ratio, crystalline products with different compositions, structures and morphologies have been obtained.

Nanocrystalline dispersions of titanium dioxide, either of the hydrothermal or any other origin, are very efficient for the photocatalytic degradation of various pollutants. However, photocatalytic reactions utilizing the slurried form of catalyst are burdened by the need for catalyst recovery. Therefore, photocatalyst immobilised onto suitable support is usually the preferred form for practical application. Although titania coatings have been fabricated by countless different processes, wet coating techniques constitute a very popular approach. At the same time, hydrothermally synthesized nanocrystalline titania dispersions are excellent raw materials for wet coating formulations, providing a good level of control over the crystallinity of the resulting layer.

Many different wet-coating techniques have been proposed, such as dip-, spin- or spray-coating, doctor blade spreading, roller etc [28]. However, recently a new promising wet coating technique has become available. This novel approach is usually termed inkjet material deposition or shortly material printing. The technique shares the basic principles with conventional inkjet printing, i.e. tiny droplets of a low-viscosity liquid are precisely deposited onto a substrate by means of thermal or piezoelectric printhead. In the case of material printing, the ink is a specially formulated liquid used for transporting a functional component onto the substrate surface [29–33].

Material printing has been successfully employed for the deposition of a great variety of functional materials, titanium dioxide including. Generally, two different approaches can be identified when discussing titania printed layers: The printing "ink" can be based on the sol–gel chemistry utilizing an organometallic precursor in the form of stable sol. Printed ink dries to form a xerogel layer which is further processed into oxide layer usually by calcination at 300–500 °C [34–40]. The second route relies on the formulation of stable colloidal suspension of nanocrystalline TiO_2 followed by a delivery of this suspension onto substrate by means of the inkjet printing [41–47]. Naturally, the free-standing nanoparticles have only very limited adhesion to substrate and need to be fixed e.g. by heat sintering or the addition of suitable binder [48].

In this paper, we report the influence of different hydrothermal conditions on the physical properties and photocatalytic activity of prepared TiO_2. Hydrothermally prepared titania slurries were deposited onto soda-lime glass substrates by material printing and effect of layers thickness was investigated.

2. Experimental

2.1. Hydrothermal synthesis of TiO_2

Colloidal dispersion of titanium dioxide was prepared by hydrothermal synthesis using titanium oxochloride($TiOCl_2$) as a precursor. $TiOCl_2$ was added dropwise to 480 mL of potassium hydroxideaqueous solution with concentration 5 mol L^{-1} to neutral reaction. KOH was used as the precipitation agent. Mixture was washed several times to remove excess of chloride ions which can have a negative influence on final TiO_2 photocatalytic activity [49]. According to our previous finding, acidic environment is much better for photocatalytic activity of colloidal TiO_2 than basic medium [50]. So HCl (p.s.)(0.9 mL) was added to TiO_2 mixture for decreasing final pH value to 1. The mixtures were hydrothermally treated under different conditions. The influence of temperatures and duration of hydrothermal synthesis on the final properties of prepared samples was investigated. We used temperature 110 °C and 160 °C. These particular temperatures were selected arbitrarily to include samples processed at a temperature close to the boiling point of water (which is favourable from the practical engineering and energy consumption point of view) and a sample set processed at a significantly higher temperature. According to our previous experience the difference of 50 °C was expected to be sufficient to induce significant differences in the properties of prepared samples. Treatment duration was 6 h, 24 h and 48 h yielding 6 samples of nanocrystalline titania dispersions.

2.2. Thin layer printing

Soda-lime glass platesof size 50 mm × 50 mm × 1.1 mm were used for TiO_2 immobilization. Firstly, it was necessary to pre-treat the soda-lime glass plates in sulphuric acid in order to prevent sodium ions diffusion which would have caused a reduction of photocatalytic activity [51,52]. Just after and before the layer coating, the plates were washed in an aqueous surfactant solution to remove of dust, grease and other residues which might have contaminated the surface during plate storage.

Titania application was performed in an innovative way utilizing an experimental printer FUJIFILM Dimatix (Dimatix Materials Printer DMP-2831). In order to fully exploit the full potential of this device, printing inks needed to be formulated and optimized proving stable and reliable jetting:1 mL of hydrothermally synthesized TiO_2dispersion was mixed with 1 mL HCl (p. s.) and 1 mL surfactant (see Section 3.4. for surfactant choice discussion) and 1 ml H_2O, respectively.

The prepared formulation was stable and was used directly as the printing ink. Before filling the cartridge ink tank, it was necessary to sonicate the ink for 5 min and filter it through a 0.45 μm size syringe filter in order to eliminate any aggregates and solid contaminants which may clog the printhead nozzles.

The Dimatix 10 pL printhead containing 16 nozzles was attached to the filled ink tank and mounted into the Dimatix printer. The nozzle temperature was set to 40 °C which was beneficial for further viscosity reduction without increasing the evaporation rate from printing nozzles too much. Nozzle span was set to 20 μm, i.e. 2500 drops per mm^2. Dimatix model liquid 2 waveform was used and the piezo driving voltage was set to 22 V.

One-layer and two-layer samples were coated by this method for all six samples. The printing of two layers was performed in the so called "wet-to-dry" manner, meaning that the first layer was completely dry before printing the second one. Simultaneously with the synthesized TiO_2, we printed also one- and two-layer samples with an ink prepared from commercial TiO_2 (Evonik Aeroxide P-25) which was used as a comparative standard. A simple 4 cm square pattern was printed in the middle of the 5 cm square glass plate. Finally, the printed substrates were placed into a calcination furnace and printed titania layers were fixed by heating with a ramp of 3 °C/min and keeping at 500 °C for 30 min.

2.3. Characterization

Crystallinity of TiO_2 was examined from X-ray powder diffraction pattern measurement by using Cu Kα as the radiation source. We used X-ray diffractometer Empyrean, Panalytical for this analysis. The titania powder was prepared by drying the hydrothermally synthesized colloidal dispersion at the temperature of 50 °C to constant weight.

Subsequently, the crystallite size was calculated using Scherrer Eq. (1), where B is constant equal 0.94, λ is the wave length which is equal to 1.54 Å and β is the width of peak at a half of maximal height.

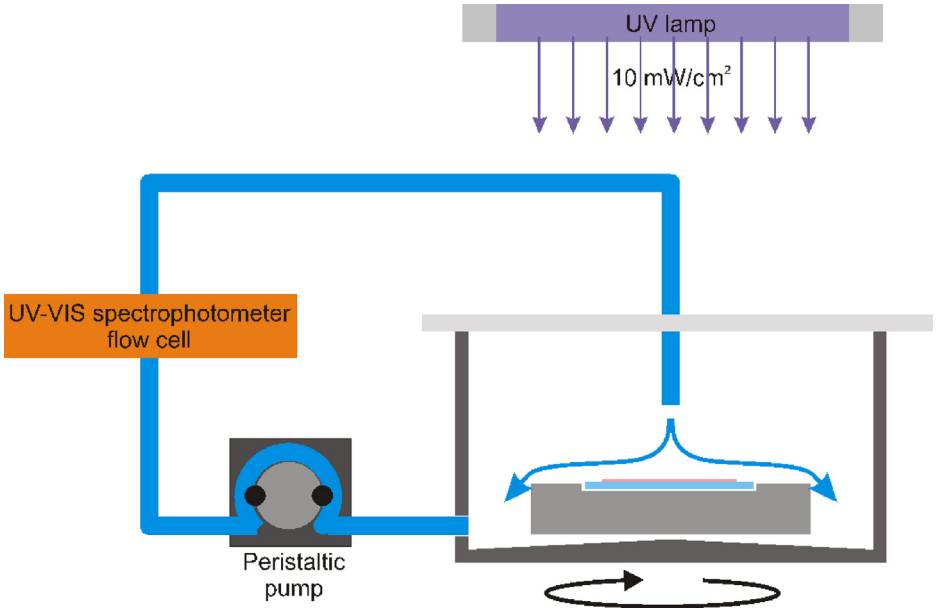

Fig. 1. Arrangement of photocatalytic reactor.

The influence of different time, temperature and pH of process was studied.

$$d = \frac{B \cdot \lambda}{\beta \cdot \cos\theta} \quad (1)$$

Transmission electron microscopy (TEM) was used for the analysis of prepared TiO_2 crystallite size as well as their shape. We used a JEOL JEM 2010 microscope operated at 200 kV, equipped with a LaB_6 tip. The samples were prepared by simply putting a drop of the solution containing the particles on a holey-carbon thin film supported on a microscopy copper grid.

The band gap of the prepared TiO_2 was evaluated from diffused reflectance measurement. We used fiber UV–vis spectrometer equipped with two lamps, deuterium lamp for UV region and halogen lamp for VIS area. The optical path consists of several optical fibers where six of them are connected with the lamps providing illumination of the sample and one reading fiber connected to the spectrometer. Reflectance was measured in the range of wavelength from 290 nm to 500 nm and barium sulfate was chosen as a reference. Molar absorption coefficient was calculated using the following formula (1), which is derived from Kubelka-Munk theory where α is molar absorption coefficient and R is reflectance.

$$\alpha = \frac{(1-R)^2}{2R} \quad (2)$$

Direct as well as indirect transitions were examined. For direct transition, the dependence of $(\alpha{\cdot}h{\cdot}\nu)^2$ on $(h{\cdot}\nu)$ is plotted where $(h{\cdot}\nu)$ is the photon energy. On the other hand, $(\alpha{\cdot}h{\cdot}\nu)^{1/2}$ as a function of photon energy was plottted for the indirect transition, and we calculated the band gap energy from extrapolation of molar absorption coefficient to zero [53].

The amount of deposited TiO_2 particles was determined by gravimetric method. We measured the weight of glass substrate before printing and then after thermal fixing of the printed titania layer. Consequently, all prepared samples were imaged by optical microscopy where we evaluated their homogeneity. Nikon Eclipse E200 microscope was used for this purpose. Images were recorded by a digital camera Nikon D5000 mounted on the optical microscope. The quality of one-layers as well as double-layers was compared.

Hardness of prepared titania films was studied by "Pencil hardness test" according to standard ISO 15184 [54]. The pencils differed in their hardness. Today there are 17 degrees of the hardness, from 9H what is the hardest to 9B what means the softest. The hardness of the layer is the same as the hardness of the pencil which does not cause any defect on its surface. This method was chosen because it is very rapid and inexpensive. On the other hand only smooth surfaces are useful and this method is destructive technique.

The surface topology of prepared layers was studied by atomic force microscopy AFM. Veeco Di CP-II (Dymek, Japan) machine in a tapping mode was used for this purpose. Images from scanning electron microscopy were received from MIRA II LMU machine by Tescan and by this analysis we examined the surface morphology of prepared thin layer of TiO_2.

2.4. Photocatalyticactivity

Photocatalytic experiments were performed in aqueous solution of 2,6-dichloroindophenol (DCIP) with an initial concentration of 2×10^{-5} mol L^{-1}. The sample was placed into a circulated batch reactor featuring a rotary sample holder (Fig. 1). Each sample was irradiated before the photocatalytic reaction by UV radiation with intensity 7.5 mW cm^{-2} for 10 min in order to activate the titania photocatalysts. UV radiation was provided by Philips Metal-halide lamp HPA 400/30 SD. The intensity was measured by Gigahertz Optic X97 Irradiance meter with X9-7 probe. Consequently, 70 mL of reaction solution was poured into the reactor and the reactor chamber was immediately covered by a UV-transparent PE foil to prevent solution evaporation. Continuous flow of the model substance was maintained by a peristaltic pump. Due to the circular movement of the sample holder the model solution was evenly spread over the whole active surface and a constant thickness of the liquid film was maintained during the whole reaction. SpectraSuite Ocean Optics software of fibre spectrometer provided on-line data collecting every 1 min. Change of DCIP concentration was determined at 600 nm. All experiments ran for 40 min.

3. Results and discussion

3.1. XRD analysis

The X-ray diffraction patterns of the systems allowed us to identify the crystal phase in TiO_2 systems. All studied powders were

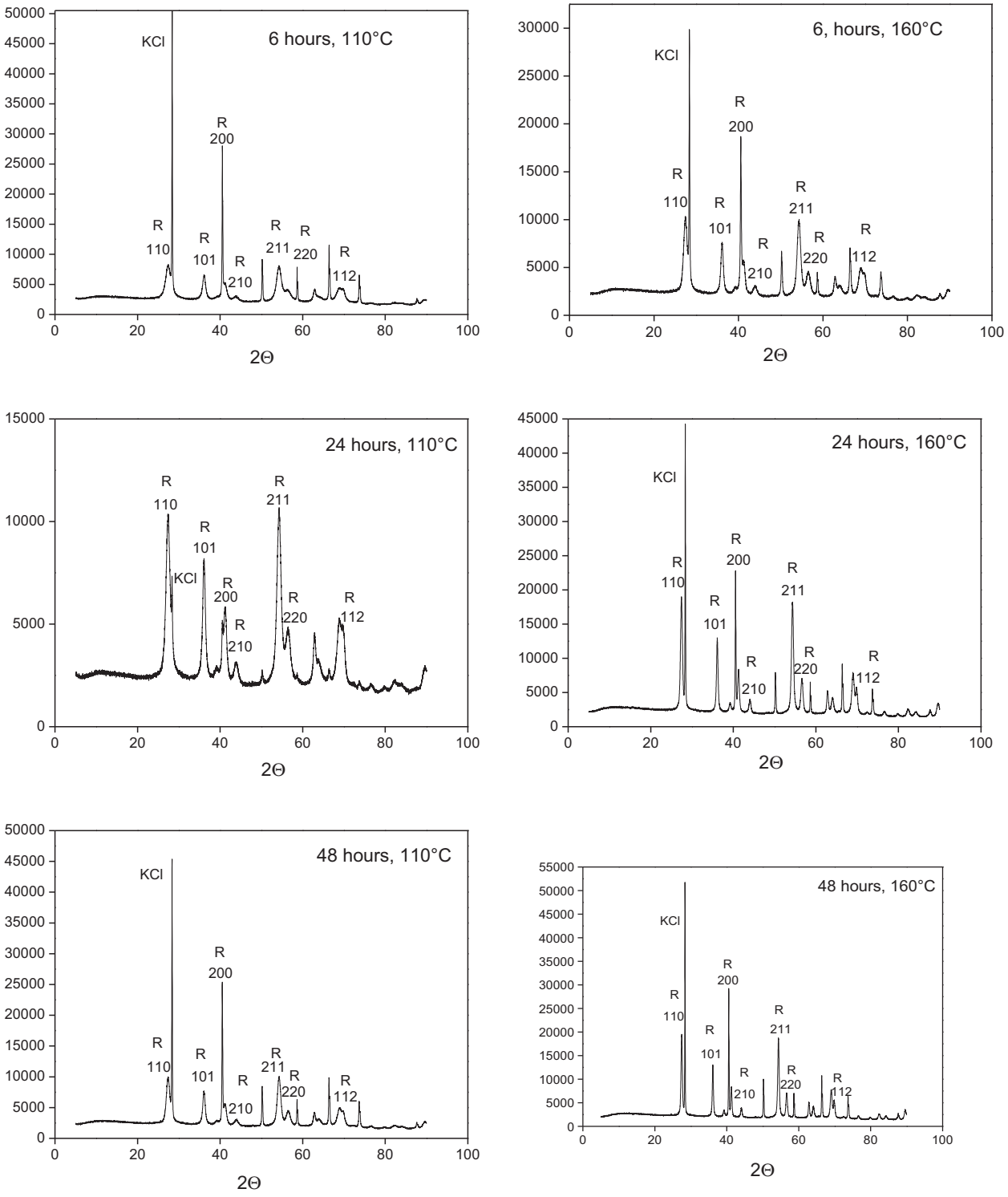

Fig. 2. XRD spectra of raw TiO_2 powders obtained from slurries synthesized at 110 °C (left) and 160 °C (right).

pure rutile (Fig. 2). This result indicates that the final crystallite phase is mostly dependent on pH, in less extent on the treatment temperature and time of hydrothermal synthesis. All investigated samples were prepared at pH 1 in contrast to the previous work [50] where TiO_2 was prepared at pH 2. This pH decreasing brought about change of TiO_2 crystallite phase from mixture of anatase and rutile to pure rutile. This result is in good agreement with published data of Yin et al. [55] where they observed that pure rutile is obtained at lower temperature of hydrothermal synthesis using pH around 1.

We can also observe quite intensive peak for KCl which could remain in the samples due to the insufficient washing of titania slurries.

Crystallite sizes were calculated using Scherrer Eq. (1). Obtained results are summarized in Table 1. We can observe that crystallite size decreases with increasing time of hydrothermal

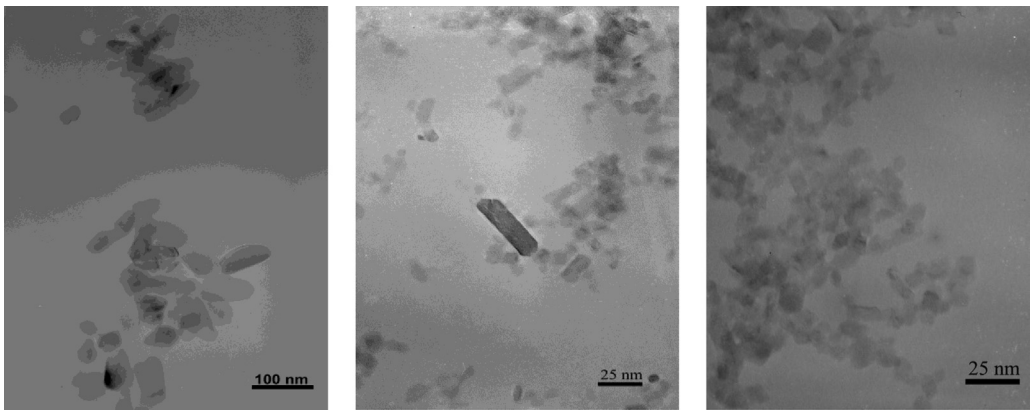

Fig. 3. TEM images of TiO_2 synthesized at 160 °C; 6 h (left), 24 h (middle), 48 h (right).

Table 1
Crystallite size (nm).

110 °C			160 °C		
6 h	24 h	48 h	6 h	24 h	48 h
12 nm	10 nm	9 nm	26	20	12

synthesis. This dependence was observed for both temperatures.

3.2. Transmission electron microscopy

Transmission electron microscopy shows that particle size decreases with increasing time of hydrothermal synthesis. We also studied the shape of prepared titania particles. We can observe rods (Fig. 3) which is typical shape for rutile phase of TiO_2.

3.3. Evaluation of band gap

Absorption coefficient was calculated according Eq. (2)from reflectance measurement (Fig. 4) and consequently used to establish the type of band-to-band transition in these TiO_2 nanoparticles. The dependence of molar absorption coefficient was recorded as a function of the photon energy for direct as well as for indirect transition (Fig. 5). Subsequently, the extrapolation for value $\alpha = 0$ was performed from which the band gap energy was found. Generally, it is known that band gap energy of TiO_2 in anatase phase is 3.23 eV and rutile phase 3.03 eV. Results summarized in Table 2 show that all prepared TiO_2 were direct semiconductors.

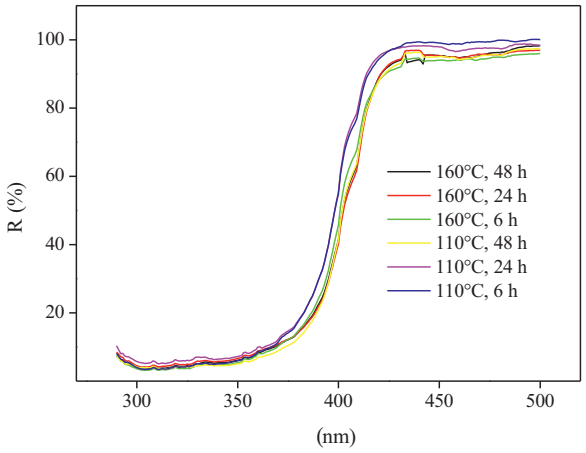

Fig. 4. Result from reflectance measurement of powder TiO_2.

3.4. Preparation of thin layers by inkjet printing

Hydrothermally synthesized TiO_2 was deposited onto soda-lime glass plates by material printing. Titania dispersions were used for the formulation of water based printing inks. Organic solvents are generally more preferred for industrial inkjet formulations because of greater possibilities to control wetting, evaporation rate and nozzle drying issues, but their use is accompanied by greater environmental impact (VOC emissions, waste disposal etc.). Water was therefore chosen as a greener alternative in this case.

Because TiO_2 particles can aggregate which would cause the problem with clogging of printed head nozzle and consequently their damage we have to avoid the aggregation by adding a surfactant. Three different surfactant Fig. 6 were tried; non-ionic surfactant (Tween 20), cation active surfactant (CTAB) and anion active surfactant (Dodecylbenzene Sulfonic Acid, Abeson). We found that only anion active surfactant has the required effect and the aggregation of colloidal particles was completely suppressed. Non-ionic (Tween 20) leaded to decreasing of aggregation but in insufficient extend. CTAB caused the precipitation of titania particles from the solution. Therefore all samples were printed using an anion active surfactant. HCl was added in order to maintain the required pH providing the surface charge of titania particles. Abeson, being a surfactant with anion-active character, is thus capable of effective stabilization of positively charged colloidal particles of TiO_2. Water was added to reach the optimum viscosity of the printing formulation (10 mPa s). Viscosity is one of the key properties that determine the printability. Wetting ability, i.e. the printing ink surface tension, plays also an important role in both the jetting process as well as the wet layer formation. Reasonably good wetting even on glass surface was provided by the relatively high surfactant concentration.

The stability of prepared TiO_2 colloidal dispersions was an issue of a previous study [50]. The stability of used printed mixtures was

Table 2
Summarised of band gap energy.

Temperature	Time	Direct transition	Indirect transition
110 °C	6 h	3.019 eV	3.348 eV
	24 h	2.984 eV	3.272 eV
	48 h	2.983 eV	3.282 eV
160 °C	6 h	2.990 eV	3.319 eV
	24 h	2.972 eV	3.303 eV
	48 h	2.977 eV	3.274 eV

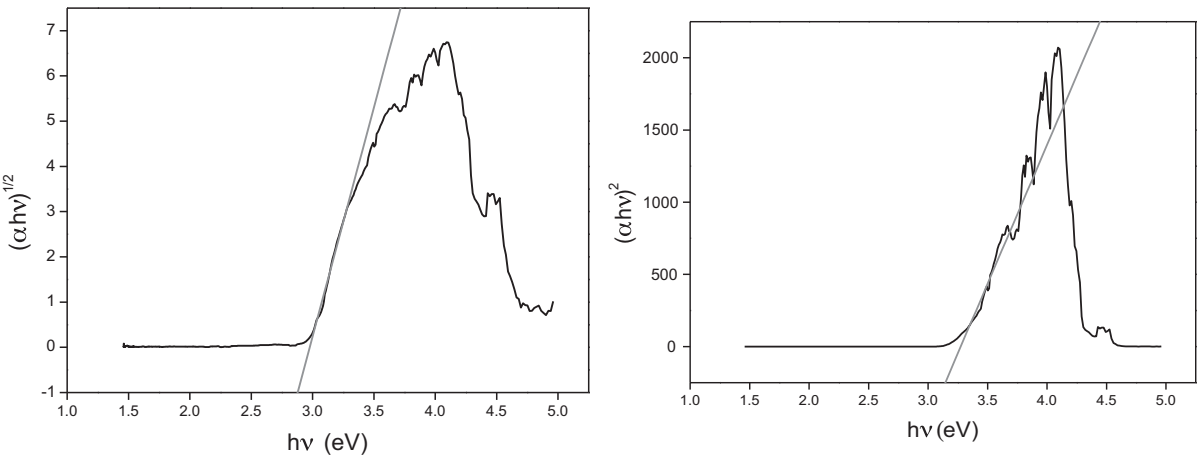

Fig. 5. Evaluation of band gap energy from direct transition (left) and indirect transition (right) for sample 160 °C, 48 h.

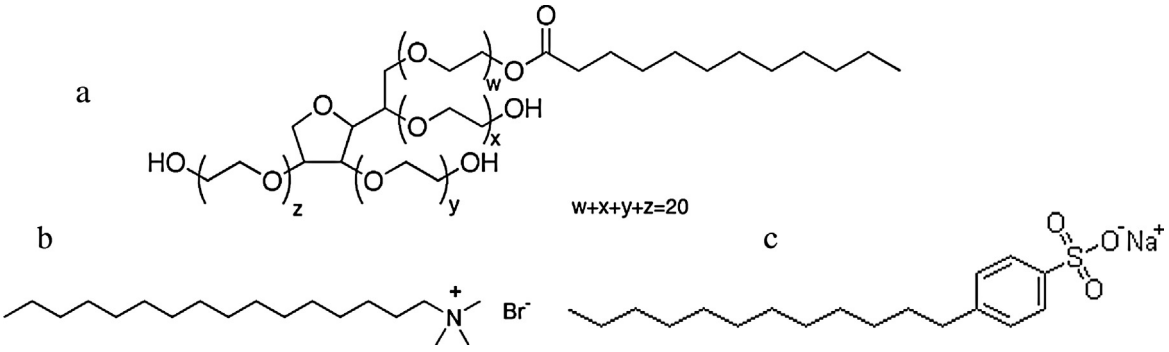

Fig. 6. Used surfactant, (a) non-ionic Tween 20, (b) cation active CTAB, (c) anion active Abeson.

sufficient because any sedimentation was not observed during 1 month of storage. All prepared samples were consumed within this time so no further data on stability is available.

Since one-layered as well as double-layered films of TiO_2 were prepared, the influence of layers thickness on the final photocatalytic activity was investigated apart from the time and temperature variables of the hydrothermal process. All prepared films were fixed on the substrate drying at temperature 500 °C for 30 min. This final heat treatment is necessary in order to remove the non-volatile organic fraction of the printing formulation (i.e. the surfactant), to sinter the titania particles together and to provide sufficient adhesion to the glass substrate.

3.5. Gravimetric analysis

The amount of TiO_2 particles deposited onto soda-lime glass was examined by gravimetric measurement of the substrate before and after the printing process. The obtained results are summarized in Table 3. We confirmed that in the case of double-layers the amount of deposited titania increased twice. This result indicates that deposition process was stable and reliable during the whole printing process and no nozzle clogging took place.

Table 3
Total amount of deposited TiO_2 per 16 cm^2 sample area.

Temperature	Time (h)	1 layer (g)	2 layer (g)
110 °C	6	0.0015	0.0028
	24	0.0012	0.0023
	48	0.0015	0.0030
160 °C	6	0.0011	0.0021
	24	0.0011	0.0026
	48	0.0008	0.0020
P-25		0.0006	0.0014

3.6. Optical microscopy

The quality of prepared layers was investigated using Nikon Eclipse E200 optical microscope connected with a digital camera Nikon D70. 20× magnifying lens were used. This was sufficient because the main purpose of this imaging was to monitor the homogeneity of prepared layers. The TiO_2 films deposited on soda-lime glass plates by material printing method show milky colour and they adhered well to the glass substrate after the fixing process. All prepared layers were quite compact and homogeneous without any noticeable cracks. All double-layers were darker which was caused by higher amount of TiO_2 in the layers (Fig. 7). No significant difference was observed using different hydrothermal conditions.

3.7. Investigation of layers hardness

The hardness of titania layers was examined by "Pencil Hardness test" according to standard ISO 15184. This study was carried out only for two-layer samples where we supposed lower adhesion than in case of one-layers. The test was performed using a mechanical device.The pencils with different hardness were used and we studied the extend of caused damage. We can observe defect in titania layer caused by pencil with hardness HB in Fig. 8. However no defect is obvious using pencil with hardness B (Fig. 8). These results indicate that the hardness of our layers corresponded to "B" pencil hardness.

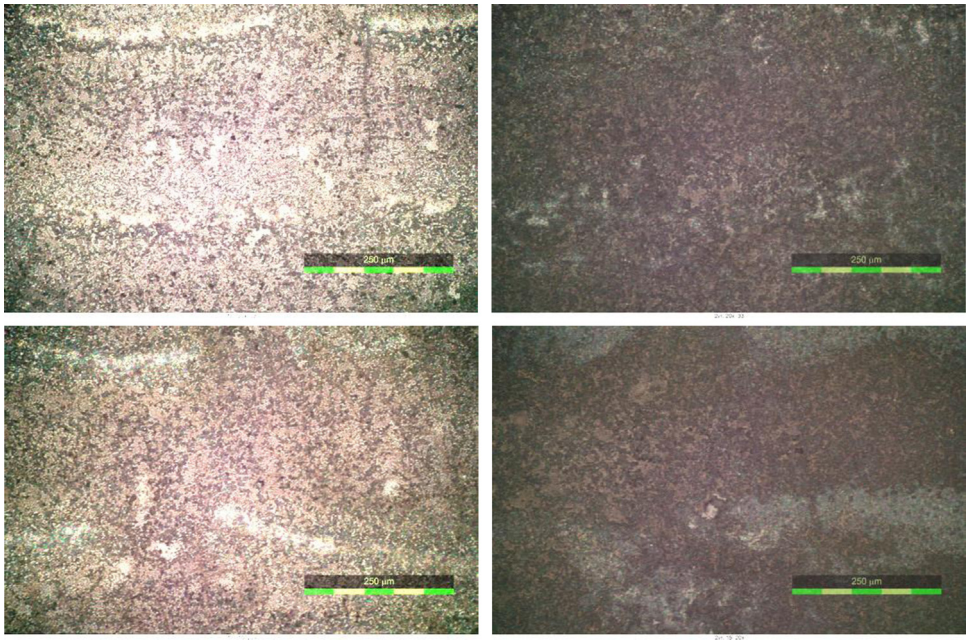

Fig. 7. Images from optical analysis, top–synthesizes at 160 °C for 6 h, 1 layer (left) and 2 layers (right); bottom. synthesized at 110 °C for 48 h, 1 layer (left) two layer (right).

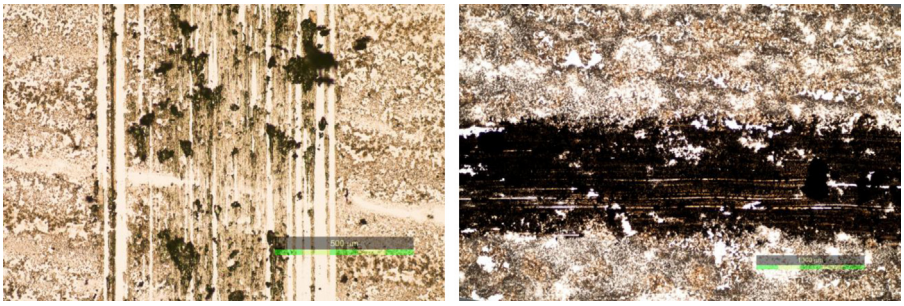

Fig. 8. Titania layers after pencil hardness test for HB pencil hardness (left) and B pencil hardness (right).

3.8. Scanning electron microscopy

The morphology of titania printed layers was studied by SEM analysis. The grain size of TiO_2 and the homogeneity of prepared layers were compared for samples synthesized under different conditions. This analysis confirmed that with increasing time of hydrothermal treatment the homogeneity of printed layers increased (Fig. 9). It is in a good agreement with the results from TEM analysis (Fig. 3). The grain size of each sample was evaluated and we found that the grain size decreases with increasing time of treatment. These results were observed for both temperatures.

3.9. Atomic force microscopy

We confirmed the result from SEM measurements by AFM analysis where we observed that with increasing time of hydrothermal treatment the grain size decreases (Fig. 10). The comparison of grain sizes was carried out from scans across 1 μm^2 area. We also examined the roughness of prepared layers from 25 μm^2 area. Roughness (R_q) increases with increasing time of hydrothermal treatment (Table 4).

3.10. Photocatalysis

The photocatalytic activity was evaluated as the rate of DCIP degradation reaction carried out in a circulated batch reactor. The degradation of DCIP takes place in several steps. The first one is dechloration which is accompanied by discoloration. Consequently, the oxidation of the carbon skeleton occurs which leads to the formation of short-chain carboxylic acids. Finally, these acids undergo decarboxylation and are totally cleaved to CO_2 and water [56–59]. Decolourization can be conveniently measured as absorbance decreasing by UV–vis spectroscopy. This method is very attractive for the purpose of studying photocatalytic activity due to its low demands for instruments and labour. Nevertheless, the authors are well conscious of the problems inherently associated by using any dye molecule: dye molecules are complex systems and during their degradation many intermediates compete for oxidation by reactive oxygen species [60,61]. From the scientific point of view, the use of simple molecules such as formic acid or dichloroacetic acid would be preferable [62]. On the other hand

Table 4
Roughness of titania printed layers.

Temperature	Time (h)	Roughness (nm)
110 °C	6	40
	24	84
	48	91
160 °C	6	60
	24	53
	48	105

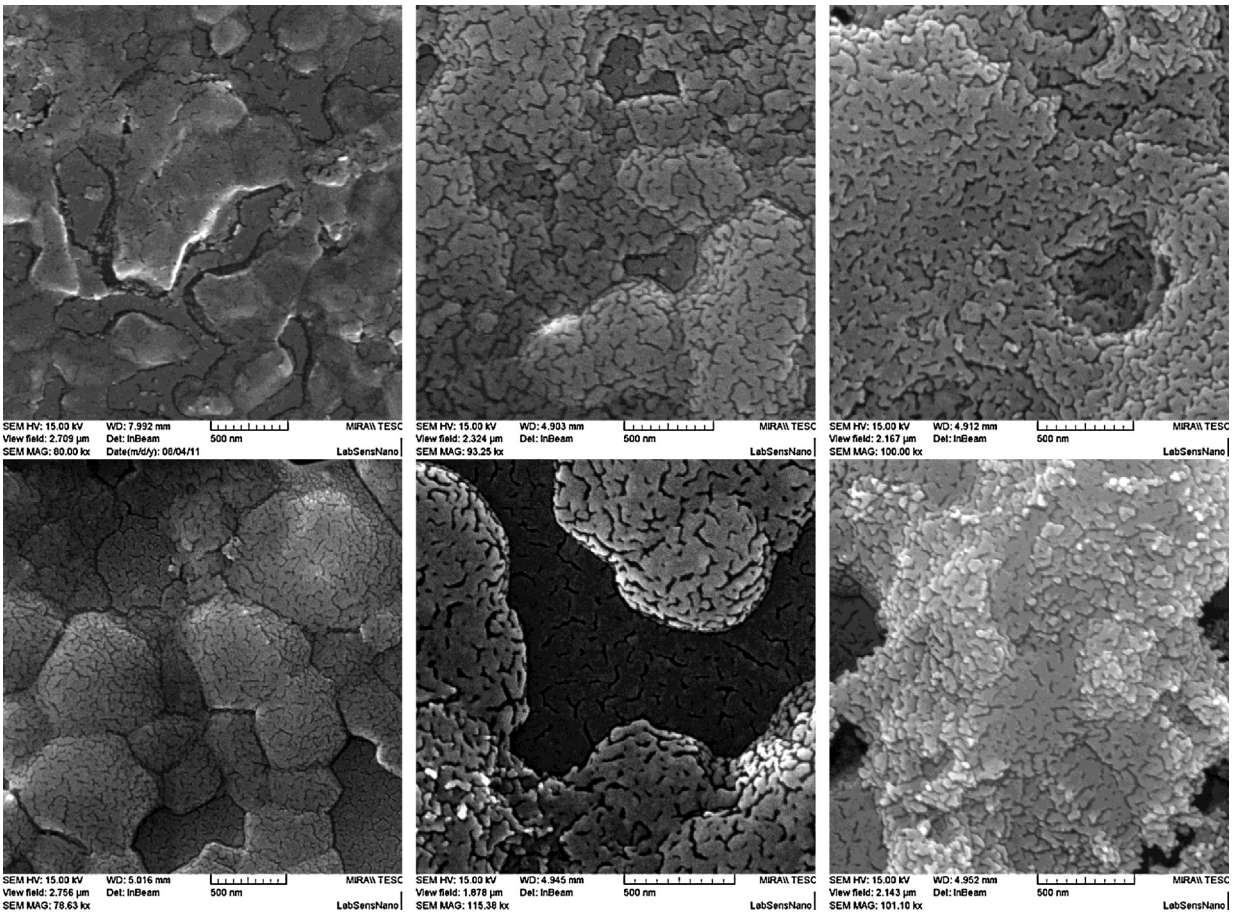

Fig. 9. SEM images for one- layers samples of titania synthesized at 110 °C (top) and 160 °C (bottom) for different time; 6 h (left); 24 h (middle); 48 h (right).

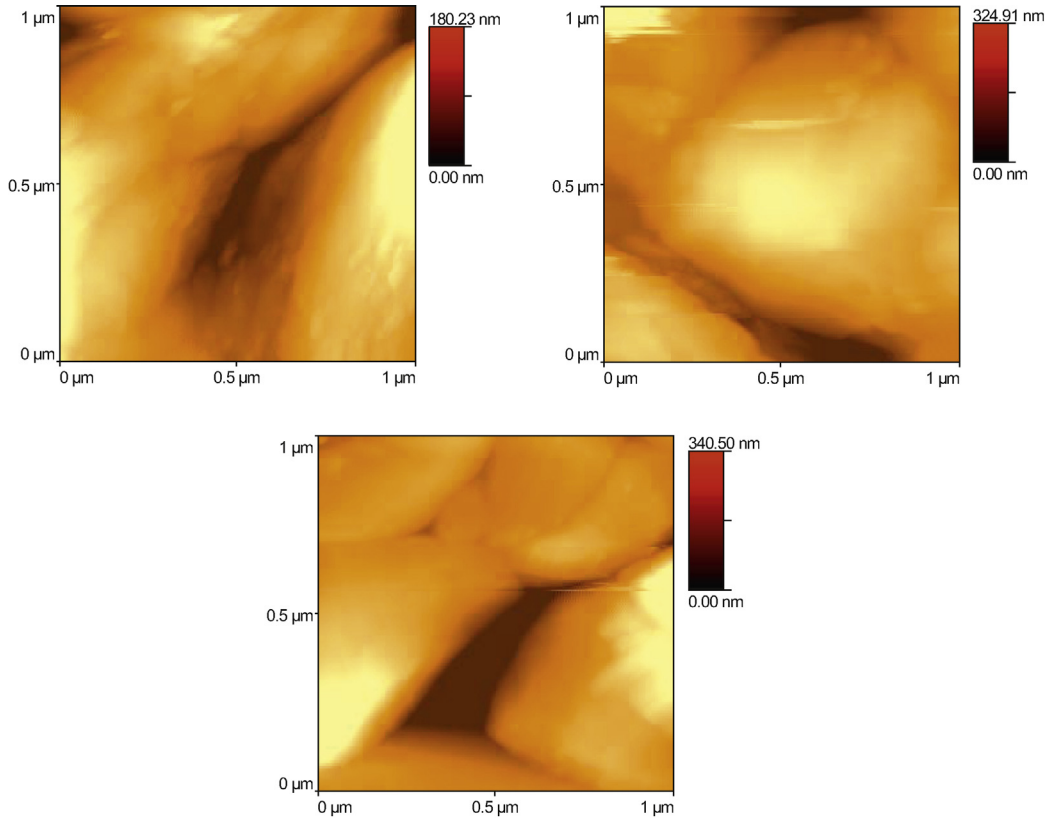

Fig. 10. Images form AFM analysis, comparison of titania grain size treated for different time; 6 h (left, top); 24 h (right, top), 48 h (left, bottom).

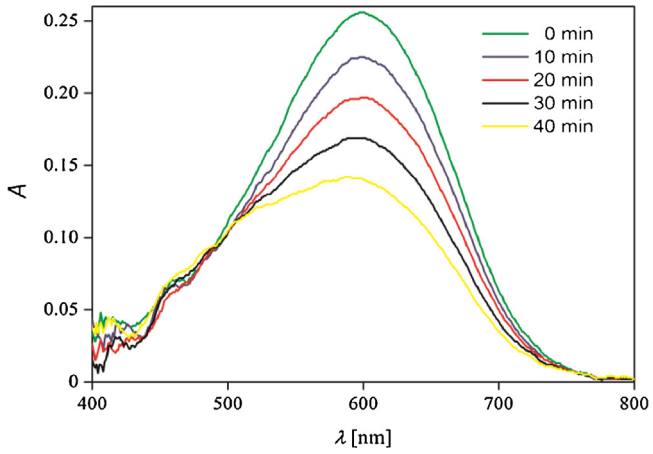

Fig. 11. Absorption spectrum of DCIP during 40 min of degradation.

Table 5
Formal 1st order rate constant, their standard errors and conversion degree for experiment took place using intensity 7.5 mW cm^{-2}.

Sample			k (min^{-1})	SE (min^{-1})	Conversion degree (%)
110 °C	6 h	1 layer	0.0002	0.0001	51.0
		2 layers	0.0090	0.0005	66.4
	24 h	1 layer	0.0049	0.0003	61.6
		2 layers	0.0163	0.0009	74.9
	48 h	1 layer	0.0130	0.0007	69.6
		2 layers	0.0212	0.0012	79.2
160 °C	6 h	1 layer	0.0084	0.0005	68.6
		2 layers	0.0083	0.0005	67.4
	24 h	1 layer	0.0122	0.0008	72.8
		2 layers	0.0153	0.0009	76.3
	48 h	1 layer	0.0271	0.0015	83.1
		2 layers	0.0313	0.0017	86.0
P-25		1 layer	0.0284	0.0017	84.5
		2 layers	0.0344	0.0019	87.7

the choice of DCIP is relevant because the treatment of dye-polluted waste water is one of the target application fields for photocatalytic process. Moreover, DCIP is a good model dye molecule because of an easy spectrophotometric detection and also a reasonably low absorption at wavelengths 360–400 nm.

The absorption maximum of DCIP is at wavelength of 600 nm (Fig. 11). 70 mL of DCIP with initial concentration of 2.5×10^{-5} g L^{-1} was used for photocatalytic experiments. Absorbance was recorded each minute and total reaction time was forty minutes which was sufficient for a total discoloration of DCIP. The influence of amount of TiO_2 (comparison one- and two-layers) as well as time and temperature of hydrothermal treatment was investigated. The photocatalytic activity was compared with common commercial TiO_2 (Evonik Aeroxide P-25). A blank experiment (no catalyst) was performed and its rate constant was subtracted from the obtained rate constants of prepared titania printed layers in order to correct the rates for direct photolysis of DCIP.

The dependence of natural logarithm of relative concentration versus reaction time was linear for all prepared titania layers (Fig. 12). So we assumed that reaction runs according the first order kinetics within the studied range. The reaction rate constants (k), their standard errors (SE) and conversion degree were calculated (Table 5).

The analysis was performed with intensity 7.5 mW cm^{-2}. We found out that the double-layered samples were more active. This result was supposed because of higher presence of TiO_2 in the double-layers, i.e. more photocatalyst and so higher amount of photoactive sites.

Although the amount of deposited TiO_2 in case of double-layered samples increased twice (Table 3) we did not observe

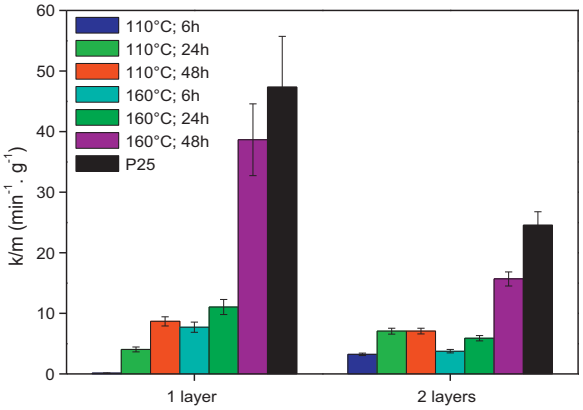

Fig. 13. Photocatalytic activity per gramof photocatalysts.

increasing of photocatalytic activity two times. It means that not all titania particles participated in the photocatalytic degradation process. This can be caused either by insufficient intensity of incident radiation and resulting self-shadowing of the thicker photocatalyst layers or by limited access of DCIP to deep buried catalyst particles resulting into mass-transfer limiting the reaction rate.

When we compared TiO_2 hydrothermally treated for different time we discovered that samples synthesized for longest time were the most active (Fig. 13, Table 5). It could be caused by the decreasing of particle size with increasing of treated time which was found by TEM and SEM analysis and also by increase of

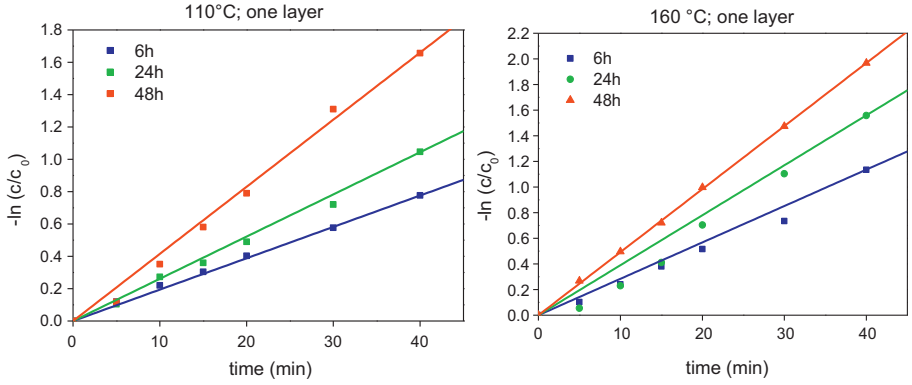

Fig. 12. Dependence of ln (c/c_0) on time for one layer samples (110 °C and 160 °C).

roughness (Table 4). Smaller crystallite size leads to higher specific surface area and to increasing of photocatalytic activity [63].

In order to compare the relative efficiency of all prepared samples, the observed photocatalytic activities were related per 1 g of photocatalyst (Fig. 13). The final standard error of these related values is influenced by the SE of both partial measurement (calculation of constant rate and SE of weighting). Final standard error was calculated according the equation (3) [64] where SE_k is standard error of calculated rate constant, SE_m is standard error of the mass and $SE_{k/m}$ is final standard error of the rate constant per 1 g of photocatalyst. When the considered values are independent r is equal to 0. When there is a total dependence r is equal 1. Because the rate constant is dependent on the amount of photocatalysts only in a small range and consequently it is independent we considered r equal to 0

$$\left(\frac{SE_{k/m}}{k/m}\right)^2 = \left(\frac{SE_k}{k}\right)^2 + \left(\frac{SE_m}{m}\right)^2 - 2r\left(\frac{SE_k}{k}\right)\left(\frac{SE_m}{m}\right) \quad (3)$$

P25 was the better photocatalyst than our samples. Most of prepared samples had activity much lower than P25, only TiO_2 synthesized for 48 h at 160 °C showed a comparable activity.

This difference between our TiO_2 and P25 was probably caused by the different phase of TiO_2. In case of P25 there was mixture of anatase and rutile however all our titania were pure rutile. So this result was expected because it is well known that mixture of anatase and rutile is much more active than only pure anatase or pure rutile.

4. Conclusion

Six TiO_2 colloidal dispersions were synthesized by the hydrothermal process. We investigated the influence of process conditions on their material properties. TEM analysis shows that particle size decreased with increasing time of synthesis. In all cases, pure rutile was prepared that implies that neither time nor temperature of hydrothermally treatment have significant influence on the final crystalline phase. Phase depends mainly on the pH used and it was the same in all samples in this study. Using a less acidic pH level (2–3) would probably result into the formation of a mixture of anatase and rutile or pure anatase. Another process parameter which could lead to the creation of rutile phase is possibly insufficient washing of the primary slurry. From the band gap energy analysis we found out that all prepared TiO_2 samples were direct semiconductors.

Consequently, synthesized TiO_2 dispersions were used for the formulation of stable "inks" and deposited onto soda-lime glass plates by inkjet printing. Only anion-active surfactants could be used for preparation of stable printing formulations. One-layered and two-layered samples were prepared and fixed by heating to 500 °C.

The quality of prepared layers was investigated by optical microscopy. The layers of TiO_2 were homogeneous, compact without any cracks. The adhesion of these layers corresponds to B pencil hardness. The morphology and particle size were evaluated by SEM and AFM analysis. We observed decreasing particle size with increasing duration of hydrothermally synthesis. This result confirmed the result from TEM analysis.

In all cases, the photocatalytic activity of double-layer samples was greater than the activity of single-layer ones. As far as the influence of the hydrothermal treatment conditions is concerned, the greatest photocatalytic activity was observed from the longest treated sample. However, the commercial de-facto standard catalyst Evonik Aeroxide P-25 still provided better activity than our best sample. This result was supposed because the activity of pure rutile is generally lower than the activity of pure anatase or anatase and rutile mixtures [65]. The use of less acidic environment during the synthesis of TiO_2 might be a viable option for reaching higher photocatalytic activity in future experiment. Despite average photocatalytic performace of this particular TiO_2 type, inkjet printing proved to be an efficient method for the fabrication of patterned titania films originating from nanocrystalline precursor.

Acknowledgements

Authors thank to Ministry of Education, Youth and Sports of Czech Republic for support by project OC10050 and the Czech Science Foundation for support through project 104/09/P165. Authors also appreciate the work of Jana Chomoucká who provided SEM imaging at the LabSensNano laboratory of Faculty of Electrical Engineering and Communication, Brno University of Technology. We also thank the three anonymous reviewers for valuable comments helping us to crown our work by this publication.

References

[1] M.R. Hoffman, S.T. Martin, W. Choi, D.W. Bahnemann, Chemical Reviews 95 (1995) 69.
[2] M.A. Fox, M.T. Dulay, Chemical Reviews 93 (1993) 341.
[3] J. Zhao, T. Wu, K. Wu, K. Oikawa, H. Hidaka, N. Serpone, Environmental Science and Technology 32 (1998) 2394.
[4] F.B. Li, X.Z. Li, Applied Catalysis A 228 (2002) 15.
[5] J.G. Yu, X.J. Zhao, Q.N. Zhao, Thin Solid Films 379 (2000) 7.
[6] H.G. Yu, S.C. Lee, C.H. Ao, J.G. Yu, Journal of Crystal Growth 280 (2005) 612.
[7] Y. Ding, G.O. Lu, P.F. Greenfield, Journal of Physical Chemistry B 104 (2000) 4815.
[8] S.J. Kim, H.G. Lee, S.J. Kim, J.K. Lee, E.G. Lee, Applied Catalysis A 242 (2003) 89.
[9] A.L. Linsebigler, G. Lu, J.T. Yates Jr., Chemical Reviews 95 (1995) 735.
[10] J. Yu, H. Yu, B. Cheng, M. Zhou, X. Zhao, Journal of Molecular Catalysis A 253 (2006) 112.
[11] Q. Xiang, J. Yu, P.K. Wong, Journal of Colloid and Interface Science 357 (2011) 163.
[12] Y.V. Kolen'ko, B.R. Churagulov, M. Kunts, L. Mazerolles, C. Colbeau-Justin, Applied Catalysis B 54 (2004) 51.
[13] A.L. Linsebigler, G. Lu, J.T. Yates, Chemical Reviews 95 (1995) 735.
[14] J. Yu, J.C. Yu, W. Ho, Z. Jiang, New Journal of Chemistry 26 (2002) 607.
[15] J.G. Yu, H.G. Yu, B. Cheng, X.J. Zhao, J.C. Yu, W.K. Ho, Journal of Physical Chemistry B 107 (2003) 13871.
[16] A. Panniello, M.L. Curri, D. Diso, A. Licciulli, V. Locaputo, A. Agostiano, R. Comparelli, G. Mascolo, Applied Catalysis B 121 (2012) 190.
[17] M. Andersson, L. Osterlund, S. Ljugstrom, A. Palmqvist, Journal of Physical Chemistry B 106 (2002) 10674.
[18] J.C. Yu, L. Zhang, Z. Zheng, J. Zhao, Chemistry of Materials 15 (2003) 2280.
[19] S.H. Elder, Y. Gao, X. Li, J. Liu, D.E. McCready, C.F. Windisch, Chemistry of Materials 10 (1998) 3140.
[20] J. Overstone, K. Yanagisawa, Chemistry of Materials 11 (1999) 2770.
[21] M.N. Ghayyal, H. Kebaili, M. Joseph, D.P. Deberker, P. Eloz, J. De Coninck, E.M. Gaigneaux, Applied Catalysis B 115 (2012) 276.
[22] Q. Xiang, K. Lv, J. Yu, Applied Catalysis B 96 (2010) 557.
[23] J. Yu, J. Xiong, B. Cheng, S. Liu, Applied Catalysis B 60 (2005) 211.
[24] J. Yu, B. Wang, Applied Catalysis B 94 (2010) 295.
[25] V.F. Stone Jr., R.J. Davis, Chemistry of Materials 10 (1998) 1468.
[26] X.Y. Chuan, M. Hirano, M. Inagaki, Applied Catalysis B 51 (2004) 255.
[27] J.A. Stride, N.T. Tuong, Solid State Phenomena 162 (2010) 261.
[28] H. Schmidt, M. Menning, http://www.solgel.com/articles/Nov00/coating.htm
[29] A.V. Lemmo, D.J. Rose, T.C. Tisone, Current Opinion in Biotechnology 9 (1998) 615.
[30] P. Calvert, Chemistry of Materials 13 (2001) 3299.
[31] P. Cooley, D. Wallace, B. Antone, Journal of Laboratory Automation 7 (2002) 33.
[32] J. Miettinen, V. Pekkanen, K. Kaija, P. Mansikkamäki, J. Mäntysalo, M. Mäntysalo, J. Niittynen, J. Pekkanen, T. Saviauk, R. Rönkkä, Microelectronics Journal 39 (2008) 1740.
[33] M. Singh, H.M. Haverinen, P. Dhagat, G.E. Jabbour, Advanced Materials 22 (2010) 673.
[34] A. Matsuo, R. Gallage, T. Fujiwara, T. Watanabe, M. Zoshimura, Journal of Electroceramics 16 (2006) 533.
[35] K.K. Manga, S. Wang, M. Jaiswal, Q. Bao, K.P. Loh, Advanced Materials 22 (2010) 5265.
[36] M. Arin, P. Lommens, N. Avci, S.C. Hopkins, K. De Buysser, I.M. Arabatzis, I. Fasaki, D. Poelman, I. Van Driessche, Journal of the European Ceramic Society 6 (2011) 1067.
[37] P. Dzik, M. Vesely, J. Chomoucka, Journal of Advanced Oxidation Technologies 13 (2010) 172.
[38] M. Cerna, M. Vesely, P. Dzik, Catalysis Today 1 (2011) 97.
[39] M. Morozova, P. Kluson, J. Krysa, P. Dzik, M. Vesely, O. Solcova, Sensors and Actuators B 160 (2011) 371.

[40] P. Dzik, M. Morozova, P. Kluson, M. Vesely, Journal of Advanced Oxidation Technologies 15 (2012) 89.
[41] S.J. Kim, D.E. Mckean, Journal of Materials Science Letters 17 (1998) 141.
[42] I. Bernacka-Wojcik, R. Senadeera, P.J. Wojcik, L.B. Silva, G. Doria, P. Baptista, H. Aguas, E. Fortunato, R. Martins, Biosensors and Bioelectronics 5 (2010) 1229.
[43] M. Yang, L. Li, S. Zhang, G. Li, H. Zhao, Sensors and Actuators B 2–3 (2010) 622.
[44] M. Arin, P. lommens, S.C. Hopkins, G. Pollefeyt, J. Van der Eycken, S. Ricard, X. Granados, B.A. Glowacki, I. Van Driessche, Nanotechnology 16 (2012) 165603.
[45] I. Fasaki, K. Siamos, M. Arin, P. Lommens, I. Van Driessche, S.C. Hopkins, B.A. Glowacki, I. Arabatzis, Applied Catalysis A 411–412 (2012) 60.
[46] Y. Oh, H.G. Yoon, S.N. Lee, H.K. Kim, J. Kim, Journal of the Electrochemical Society 159 (2012) B35.
[47] M. Hosseini Zori, A. Soleimani-Gorgani, Journal of the European Ceramic Society (2012) http://dx.doi.org/10.1016/j.jeurceramsoc.2012.06.005
[48] H. Shibata, H. Sakai, P. Rangsunvigit, T. Hirano, M. Abe, Surface Coatings International Part B: Coatings Transactions 86 (2003) 125.
[49] A. Piscopo, D. Robert, J.V. Weber, Applied Catalysis B 35 (2001) 117.
[50] M. Cerna, C. Guillard, E. Puzenat, M. Veselz, P. Dzik, International Journal of Chemical and Environmental Engineering 2 (2011) 255.
[51] J-M. Herrmann, H. Tahiri, C. Guillard, P. Pichat, Catalysis Today 54 (1999) 131.
[52] Y. Paz, A. Heller, Journal of Materials Research 12 (1997) 2759.
[53] K.M. Reddy, S.V. Manorama, A.R. Reddy, Materials Chemistry and Physics 78 (2002) 239.
[54] ISO 15184: Paints and varnishes, Determination of film hardness by pencil test, 1998.
[55] H. Yin, Y. Wada, T. Kitamura, S. Kambe, S. Murasawa, H. Mori, T. Sakata, S. Yanagida, Journal of Materials Chemistry 11 (2001) 1694.
[56] V. Brezova, M. Ceppan, M. Vesely, L. Lapcik, Chemical Papers 45 (1991) 233.
[57] D.F. Ollis, Environmental Science and Technology 19 (1985) 480.
[58] R.W. Matthews, Journal of the Chemical Society, Faraday Transactions 1 85 (1989) 1291.
[59] M. Cerna, M. Veselz, P. Dzik, Catalysis Today 161 (2001) 97.
[60] B. Ohtani, Chemistry Letters 37 (2008) 217.
[61] H. Kisch, W. Macyk, ChemPhysChem 3 (2002) 399.
[62] J. Ryu, W. Choi, Environmental Science and Technology 42 (2008) 294.
[63] D.S. Kim, S.Y. Kwak, Applied Catalysis A 323 (2007) 110.
[64] K. Doerffe, K. Eckschlager, Optimální Postup Chemické Analýzy, SNTL, Leipzing, 1998, p. 22.
[65] J. Yu, G. Wang, B. Cheng, M. Zhou, Applied Catalysis B 69 (2007) 171.